# The Effects of Crystal Size on the Lattice Dynamics of $SrTiO_3$

Scott C. Johnson* and Lawrence B. Coleman†

*University of California, Davis*

(Dated: November 13, 2001)

## Abstract

Infrared spectroscopy is used to study the lattice dynamics of polycrystalline thin films of $SrTiO_3$ with varying crystal sizes. Samples are fabricated by spin-coating a sol-gel precursor onto a silicon wafer. The size of the crystals in the samples is controlled by the time and temperature of thermal processing. The size of the crystals is determined by x-ray diffraction. Infrared transmission spectra from $10\,\mathrm{cm}^{-1}$ to $7000\,\mathrm{cm}^{-1}$ are obtained over a temperature range of 80 K to 385 K. The spectra of the crystalline samples are fit to a 4-parameter version of the Lorentz oscillator dielectric function, which gives the frequency of the soft mode. Polycrystalline samples of $SrTiO_3$ have a soft mode with the expected temperature behavior that shows a strong dependence on crystal size. This size dependence is explained using a Landau phenomenological model.

## I. INTRODUCTION

The effects of small particle size on ferroelectric properties have been investigated since the 1950s. Early measurements[1] found $T_0$ to *increase* with decreasing particle size. It is now thought that in these early experiments, the stresses due to the mechanical preparation of the small particles had a stronger effect on the ferroelectric properties than the particle size[2,3].

Most recent investigations of particle size use sol-gel techniques to synthesize the particles. Studies of $PbTiO_3$[4], $BaTiO_3$[5], $SrTiO_3$[6], and others have been done. All have found that ferroelectricity is reduced or eliminated in small particles and in thin films[7].

It is not clear why small size reduces ferroelectricity. Several mechanisms have been proposed, including lattice expansion due to the small particle size[8], contact forces between particles[3,9], and the energy cost of polarization gradients and steps (a Landau phenomenological model)[10]. Others have used a purely empirical form to fit ferroelectric polarization *vs.* particle size data[2,4,11]. We will find agreement with the Landau phenomonology.

In this paper, we study the lattice dynamics of $SrTiO_3$ as a function of crystal size and of temperature. $SrTiO_3$ is an incipient ferroelectric with soft mode behavior suggesting a ferroelectric phase transition at 40 K, but the transition never occurs[6,12,13]. We choose $SrTiO_3$ because its soft mode is underdamped and easily visible in infrared spectra. Since ferroelectricity in perovskites is determined by the behavior of the soft mode, finding the changes in the soft mode behavior caused by varying crystal size gives unique insight into the effect of crystal size on the ferroelectric phase.

## II. EXPERIMENTAL

Samples are prepared by spin coating a sol-gel precursor[14] onto silicon substrates in air. Hydrolysis with atmospheric water vapor results in a porous film. Samples are heated in air at 700 K giving dense amorphous films. Films are crystallized by heating above their crystallization temperature of approximately 800 K. Samples heated for more than 20 seconds result in approximately constant crystal sizes. Smaller crystal sizes are obtained by heating for shorter times and by hydrolyzing the films in an atmosphere enriched in carbon dioxide and water, which increases the concentration of carbonate impurities.

The average size of the crystallites in our samples is determined by x-ray diffraction. We measure our films using copper $K\alpha$ radiation ($\lambda = 1.54178$ Å using the weighted average of the $\alpha_1$ and $\alpha_2$ lines). The size of the crystallites can be determined by the Scherrer equation,

$$d = \frac{K\lambda}{w\cos\theta} \tag{1}$$

where $d$ is the diameter of the crystallites, $w$ is the full width at half maximum of the diffraction peak, $\theta$ is the angle of incidence of the x-rays measured from the plane of the sample, $\lambda$ is the wavelength of the x-rays, and $K \approx 1$ is a constant that depends on the shape of the crystallites. We use $K = 0.89$. We also correct for the broadening due to the source doublet[15], which gives corrections between 2% and 14%. The resulting size measurements for the four samples we chose for detailed study are 10 nm, 12 nm, 22 nm, and 27 nm.

The lattice constant in all of these samples is 3.90 Å $\pm$ 0.01 Å, which agrees with the single crystal value to that uncertainty. This suggests that our samples have little or no internal stress. This is reasonable to expect from sol-gel derived crystals, which typically have low internal stresses.

Transmission spectra at near normal incidence are obtained from 10 cm$^{-1}$ to 7000 cm$^{-1}$ for each sample at 300 K and over the soft mode region at several temperatures between 80 K and 385 K. Fits for these spectra are obtained by adjusting the parameters in a calculation of the transmission of a stack of parallel dielectric layers representing the silicon wafer, oxide layers, and the $SrTiO_3$ film. The interference pattern due to the parallel faces of the silicon wafer is removed from the calculated spectra by Fourier filtering, and from the measured spectra by using a fairly low resolution (8 cm$^{-1}$). The thickness of the film is an adjustable parameter in the calculation and can be determined by fitting to the interference pattern of the film, which is visible between 1500 cm$^{-1}$ and 7000 cm$^{-1}$. The dielectric function for the polycrystalline film is approximated as a homogeneous dielectric[16–18] with an effective value of

$$\epsilon = \epsilon_{\mathrm{m}} \left[ 1 - \sum_j f_j \frac{\epsilon_{\mathrm{e}} - \epsilon_{\mathrm{m}}}{L_j \epsilon_{\mathrm{e}} + (1 - L_j)\,\epsilon_{\mathrm{m}}} \right]^{-1} \tag{2}$$

where $\epsilon_{\mathrm{m}}$ is the dielectric function of crystalline $SrTiO_3$ and $f_j$ is the fraction of the volume that is occupied by inclusions that are assumed to be ellipsoidal with a depolarization factor $L_j$ and dielectric function $\epsilon_{\mathrm{e}}$. A 4-parameter factorization of a Lorentz oscillator[19–21] is used for the crystalline $SrTiO_3$ layer,

$$\epsilon_{\mathrm{m}} = \epsilon_\infty \prod_j \frac{\omega_{j\mathrm{LO}}^2 - \omega^2 + i\omega\gamma_{j\mathrm{LO}}}{\omega_{j\mathrm{TO}}^2 - \omega^2 + i\omega\gamma_{j\mathrm{TO}}} \tag{3}$$

where $\omega_{j\mathrm{TO}}$ and $\gamma_{j\mathrm{TO}}$ are the frequency and damping factor for the transverse optical phonon for mode $j$ and $\omega_{j\mathrm{LO}}$ and $\gamma_{j\mathrm{LO}}$ are the same for the longitudinal optical phonon. The soft mode frequency, $\omega_0$, can be identified by its temperature dependence. Usually, it is the lowest frequency $\omega_{j\mathrm{TO}}$ for $SrTiO_3$. However, for our smallest-crystal sample at temperatures above 225 K, the soft mode is the second lowest frequency TO mode.

Spectra for the four samples are shown in Fig. 1. The large, broad absorption feature corresponds to the soft mode. Samples with larger crystals clearly have a lower-frequency soft mode.

The squares of the soft mode frequencies, $\omega_0^2$, are plotted against temperature in Fig. 2. All four samples, regardless of crystal size, follow

$$\omega_0^2 = A\,(T - T_0) \tag{4}$$

where $A = 31\,\mathrm{cm}^{-2}/K$ is a material-specific constant and $T_0$ is the transition temperature. This is the standard soft mode temperature behavior[22]. The straight line through each set of $\omega_0^2$ *vs.* $T$ data is a least squares fit to Eq. (4) keeping $A$ constant and varying $T_0$ to minimize the fitting error.

For each sample, the slope of $\omega_0^2$ *vs.* $T$ is slightly smaller at low temperatures than at high temperatures. This is similar to (but less extreme than) the behavior seen in other data[6,13]. At low temperatures ($T < \sim 100\,\mathrm{K}$), $\omega_0^2$ *vs.* $T$ does not follow its classical $\omega_0^2 = A(T - T_0)$ behavior, but instead approaches a constant as $T \to 0$. According to Kwun, this is a quantum mechanical effect. Since this non-classical behavior is so slight in our data, we ignore this low-$T$ curvature and use all of our data points in the least squares fit to a straight line.

## III. LANDAU PHENOMENOLOGICAL MODEL OF PARTICLE SIZE EFFECT

In this section, we construct a Landau phenomenological model of the polarization in a spherical particle and use it to calculate of the dependence of transition temperature $T_0$ on particle size $d$ for $SrTiO_3$.

Following Zhong and coworkers[10], we construct a Landau model of a spherical particle of diameter $d$ with a polarization $P(r)$ that varies radially in magnitude but is uniform in direction. The free energy $F$ of this particle is expressed in powers of its polarization[10,23,24]

$$
\begin{aligned}
F \; &= \int \mathrm{d}V \; \left[\frac{1}{2}A(T-T_{0\infty})P^2 + \frac{1}{4}BP^4 + \frac{1}{2}D(\nabla P)^2\right] \\
&+ \int \mathrm{d}S \; \frac{1}{2}\frac{D}{\delta}P^2
\end{aligned} \tag{5}
$$

where $A$, $B$, and $D$ are empirically determined constants, $\delta$ is the extrapolation length (a measure of the difference between the surface and the bulk), $T_{0\infty}$ is the bulk transition temperature, $\mathrm{d}V$ indicates a volume integral, and $\mathrm{d}S$ indicates a surface integral.

Compared with a similar expression for bulk material, the gradient term and the surface term are added. Thus, the physical basis for this polarization model is that it is energetically favorable to have similar polarizations in adjacent unit cells of the crystal and minimal polarization on the surface of the particle. Non-uniform polarization in the bulk requires energy proportional to $(\nabla P)^2$ per unit volume, and the abrupt polarization change at the surface requires energy proportional to $P^2$ per unit area. The ideal polarization profile of a particle will minimize the total of all these energy terms.

The variation of the free energy with respect to the polarization,

$$\frac{\delta F}{\delta P} = A(T-T_{0\infty})P + BP^3 + D\nabla^2 P \tag{6}$$

with boundary condition

$$\frac{\mathrm{d}P}{\mathrm{d}n} = \frac{P}{\delta} \tag{7}$$

at the surface of the particle, where $n$ is normal to the surface, gives the force conjugate to the polarization. In spherical coordinates, this is

$$\frac{\delta F}{\delta P} = A(T-T_{0\infty})P + BP^3 + D\left(\frac{\mathrm{d}^2 P}{\mathrm{d}r^2} + \frac{2}{r}\frac{\mathrm{d}P}{\mathrm{d}r}\right) \tag{8}$$

with boundary condition

$$\frac{\mathrm{d}P}{\mathrm{d}r} = \frac{P}{\delta} \tag{9}$$

at $r = d/2$. If we sought the equilibrium polarization, as Zhong did, we would set the force to zero and solve for $P$. However, we seek the eigenmodes. For this, we use an equation of motion for the polarization[23,25]

$$m\frac{\mathrm{d}^2 P}{\mathrm{d}t^2} + \gamma\frac{\mathrm{d}P}{\mathrm{d}t} + \frac{\delta F}{\delta P} = 0 \tag{10}$$

where $m$ is a mass term and $\gamma$ is a damping term. Since we are investigating the paraelectric state, with little or no equilibrium polarization, the $BP^3$ term in Eq. (6) will be small so we neglect it[26]. Then, Eq. (10) becomes

$$m\frac{\mathrm{d}^2P}{\mathrm{d}t^2} + \gamma\frac{\mathrm{d}P}{\mathrm{d}t} + A(T - T_{0\infty})P + D\left(\frac{\mathrm{d}^2P}{\mathrm{d}r^2} + \frac{2}{r}\frac{\mathrm{d}P}{\mathrm{d}r}\right) = 0 \tag{11}$$

with the boundary condition of Eq. (9). This is a wave equation. The spatial part,

$$\left(\frac{\mathrm{d}^2}{\mathrm{d}r^2} + \frac{2}{r}\frac{\mathrm{d}}{\mathrm{d}r}\right)P = a^2P \tag{12}$$

with boundary condition Eq. (9) is an eigenvalue equation for $P(r)$ with eigenvalue $a^2$. Note that for the limiting case of an infinite sample, $P(r)$ will be uniform so $a^2$ will be zero, and Eq. (5) will reduce to the bulk Landau free energy. The time part,

$$m\frac{\mathrm{d}^2P}{\mathrm{d}t^2} + \gamma\frac{\mathrm{d}P}{\mathrm{d}t} + A(T - T_{0\infty})P + Da^2P = 0, \tag{13}$$

has the standard form for a Lorentz oscillator, except that the eigenfrequency is given by

$$\omega_0^2 = A(T - T_{0\infty}) + Da^2. \tag{14}$$

(Note that we have set $m = 1$ in deriving Eq. (14). Since $m$, $\gamma$, $A$, and $D$ are all empirically determined constants, this is equivalent to dividing through by $m$ and rescaling $\gamma$, $A$, and $D$.) The eigenfrequency of the soft mode has the same temperature dependence as the bulk, $A(T - T_{0\infty})$, but includes a term $Da^2$ that depends on particle size. This can also be regarded as a modification of the transition temperature,

$$T_0 = T_{0\infty} - \frac{Da^2}{A} \tag{15}$$

so that $T_0$ depends on particle size.

To determine the parameter $Da^2$, we must solve Eq. (12). Without the boundary condition, this problem is equivalent to the spatial part of the Schrödinger equation for a free particle in spherical coordinates with zero angular momentum. The solutions[27] are spherical Bessel functions. We require only the lowest energy solution

$$P(r) = P_0\frac{\sin ar}{ar} \tag{16}$$

where $P_0$ is the polarization at the center of the spherical particle and $a$ is to be determined by satisfying the boundary condition. For $P(r)$ of the form of Eq. (16), inclusion of the boundary condition leads to a transcendental equation that must be solved numerically. To obtain an analytic solution, we approximate $P(r)$ using a Taylor expansion,

$$P(r) \approx P_0 \left(1 - \frac{a^2 r^2}{6}\right). \tag{17}$$

Substituting this into Eq. (9) and solving for $a^2$ gives

$$a^2 = \frac{24}{d(d+4\delta)}. \tag{18}$$

This is the main result from our model, a particle-size-dependent modification to $\omega_0^2$. It is used in Eq. (14) and the parameters $D$ and $\delta$ are determined by fitting to data. The new transition temperature $T_0$ of Eq. (15) becomes

$$T_0 = T_{0\infty} - \frac{24D}{Ad(d+4\delta)}. \tag{19}$$

This transition temperature becomes lower for smaller particle sizes. If $T_0$ becomes lower than 0 K, no transition to a ferroelectric state is possible. Hence, for materials that have a bulk ferroelectric phase like $BaTiO_3$, this result predicts a particle-size-induced phase transition to a paraelectric state below a certain particle size threshold.

To compare our empirical $D$ with values in the literature, we must carefully consider the system of units each author uses. For example, the constant $A$ used in this work for the expression

$$\omega_0^2 = A(T - T_0) \tag{20}$$

gives the slope on on a graph of $\omega_0^2$ *vs.* $T$ and has units cm$^{-2}$K$^{-1}$. The constant $A$ used by Zhong, which we will refer to as $A_\epsilon$, gives the static dielectric constant

$$\epsilon_0 = \frac{4\pi}{A_\epsilon(T - T_0)} \tag{21}$$

and has units K$^{-1}$. (It is related to $C$ in the Curie-Weiss law $\epsilon_0 = C/(T - T_0)$ by[28] $A_\epsilon = 4\pi/C$.) Hence these two constants have similar meanings, but different values. They are related by the Lyddane-Sach-Teller (LST) equation, which is

$$\frac{\omega_{\mathrm{L0}}^2}{\omega_{\mathrm{T0}}^2} = \frac{\omega_{\mathrm{L0}}^2}{A(T - T_0)} = \frac{\frac{4\pi}{A_\epsilon(T-T_0)}}{\epsilon_\infty} = \frac{\epsilon_0}{\epsilon_\infty} \tag{22}$$

in its simplest form, for a single mode with transverse optical and longitudinal optical mode frequencies $\omega_{\mathrm{T0}}$ and $\omega_{\mathrm{L0}}$. For $SrTiO_3$, with three infrared-active modes, the LST equation gives

$$\frac{A_\epsilon(T - T_0)}{A(T - T_0)} = \frac{4\pi}{\epsilon_\infty} \frac{1}{\omega_{\mathrm{L0}}^2} \frac{\omega_{\mathrm{T1}}^2}{\omega_{\mathrm{L1}}^2} \frac{\omega_{\mathrm{T2}}^2}{\omega_{\mathrm{L2}}^2} \tag{23}$$

where $\omega_{L0}$ is the LO mode frequency of the soft mode and $\omega_{T1}$, $\omega_{T2}$, $\omega_{L1}$, and $\omega_{L2}$ are the TO and LO frequencies of the other modes. For $SrTiO_3$, the value of this ratio is $5.08 \times 10^{-6}\text{cm}^2$. Since the $A$, $B$, and $D$ terms in the Landau free energy expansion of Eq. (5) are simply added to each other, each term must separately scale the same way. So, to compare the $D$ parameter we calculate (by fitting Eq. (14) to data) to the value determined by Zhong, we multiply our $D$ by the ratio of Eq. (23).

## IV. PARTICLE SIZE ANALYSIS

A plot of $T_0$ *vs.* crystal size $d$ for the Landau model is shown as the solid line in Fig. 3. The four data points on this graph correspond to the same four samples used in Figs. 1 and 2. The parameters $D$ and $\delta$ have been chosen to minimize the mean square error between the theory curve and the four data points.

We can compare our results for $SrTiO_3$ to those of Zhong for $BaTiO_3$ and $PbTiO_3$. Using their empirical values for $D$ and $\delta$ in our model, we get the dashed and dotted lines shown in Fig. 3. $BaTiO_3$ and $PbTiO_3$ show size-induced phase transitions at $d = 48\,\text{nm}$ and $d = 3.5\,\text{nm}$ respectively, in reasonable agreement with the $d = 44\,\text{nm}$ and $d = 4.2\,\text{nm}$ predictions of Zhong. Their result is for the static polarization in the ferroelectric phase. This suggests, at least, that our dynamic model is compatible with their static model. Our parameters for $SrTiO_3$ are compared with those of $BaTiO_3$ and $PbTiO_3$ from Zhong below:

| | $A$, $\times 10^{-5}\text{K}^{-1}$ | $D$, $\times 10^{-16}\text{cm}^2$ | $\delta$, nm |
|---|---|---|---|
| $PbTiO_3$[10] | 3.1 | 5 | 3 |
| $SrTiO_3$ | 15.7 | 250 | 10 |
| $BaTiO_3$[10] | 7.4 | 1263 | 43 |

Note that the parameter $B$ is not experimentally accessible to us.

The radial polarization profiles predicted by this model are shown in Fig. 4 for the smallest and largest of our $SrTiO_3$ particle sizes.

The graphical meaning of the extrapolation length is demonstrated in these graphs. The dashed lines show a linear extrapolation of $P(r)$ from its value and slope at the surface of the particle. The extrapolation length $\delta$ is the distance from the surface at which this extrapolation reaches zero.

The graphs also show that the Taylor series approximation used in the derivation of Eq. (18) is good over the length scales in our particles. It is interesting that the polarization of smaller particles is closer to uniform than that of larger particles. A macroscopic sphere of $SrTiO_3$ would have a polarization that is quite non-uniform, smoothly approaching zero at its surface. This is different from the uniform polarization of a statically polarized sphere.

Note that, following the work of previous researchers[10,23], the depolarization field has been neglected in this model. It is unclear exactly how this affects its accuracy.

We can also fit our data to a purely empirical equation[4]. With a least squares fit to our data, this equation becomes

$$T_0 = 40\,\mathrm{K} - \frac{4716\ \mathrm{K}\cdot\mathrm{nm}}{d - 4\,\mathrm{nm}} \tag{24}$$

and is shown as the dashed line in Fig. 5. For comparison, the solid line represents the fit due to the Landau model.

The fit obtained from this model is comparable to the fit from the Landau model. From our data alone, it is not possible to tell which functional form is a better model for the particle size effect on $T_0$. The advantage of the Landau model, and the reason for its inclusion in this work, is that it provides some understanding of the size effect. The purely empirical form of Eq. (24) gives us no indication of its origin. If the Landau model is correct, we can say that the origin of the particle size effect in $SrTiO_3$ is the energy cost of (or, equivalently, the forces exerted by) polarization steps and gradients at and near the surface of the particle.

## V. CONCLUSION

We have found that in polycrystalline $SrTiO_3$, the lattice dynamics are modified from that of single crystal materials. Crystal size significantly affects the behavior of the soft mode. The soft mode retains the same temperature dependence as that of single crystal samples, but is shifted to higher frequencies. Most significantly, the soft mode frequency is highest for the smallest crystals. This can be described as a dependence of $T_0$ on the size of the crystals in the sample. This size dependence is described by a Landau phenomenological model using the polarization as the expansion parameter. In this model, gradients and abrupt changes in polarization are assigned empirical energy values. The polarization profile eigenmode for a spherical particle that minimizes the total energy is then calculated. Its eigenfrequency does indeed depend on the particle size and the resulting functional form can be fit to our data rather well using two adjustable parameters. Thus, it seems that the effect of particle size on the soft mode of $SrTiO_3$ is due to the energy cost of (or, equivalently, the forces caused by) polarization gradients and abrupt changes near the surface of the particle.

---

[*] Electronic address: `sjohnson@landau.ucdavis.edu`

[†] Electronic address: `lbcoleman@ucdavis.edu`


[1] M. Anliker, H. R. Brugger, and W. Kanzig, Helvetica Physica Acta **27** (1954).

[2] W. L. Zhong, B. Jiang, P. L. Zhang, J. M. Ma, H. M. Cheng, Z. H. Yang, and L. X. Li, Journal of Physics: Condensed Matter **5**, 2619 (1993).

[3] S. Chattopadhyay, P. Ayyub, V. R. Palkar, and M. Multani, Physics Review B **52** (1995).

[4] K. Ishikawa, K. Yoshikawa, and N. Okada, Physical Review B **37** (1988).

[5] K. Uchino, E. Sadanaga, and T. Hirose, Communications of the American Ceramic Society **72**, 1555 (1989).

[6] S.-I. Kwun and T. K. Song, Ferroelectrics **197**, 125 (1997).

[7] M. H. Frey and D. A. Payne, Applied Physics Letters **63** (1993).

[8] M. Tanaka and Y. Makino, Ferroelectric Letters **24**, 13 (1998).

[9] P. Ayyub, V. R. Palkar, S. Chattopadhyay, and M. Multani, Physical Review B **51** (1995).

[10] W. L. Zhong, Y. G. Wang, P. L. Zhang, and B. D. Qu, Physical Review B **50**, 698 (1994).

[11] M. Jinfang, Z. Guangtian, C. Qiliang, L. Jiangping, W. Xiaohui, and Z. Muyu, J. Phys. Chem. Solids **55**, 427 (1994).

[12] M. E. Lines and A. M. Glass, *Principles and Applications or Ferroelectrics and Related Materials* (Oxford University Press, 1977).

[13] I. Federov, V. Zelezny, J. Petzelt, V. Trepakov, M. Jelinek, V. Trtik, M. Cernansky, and V. Studnicka, Ferroelectrics **208–209**, 413 (1998).

[14] *Catalog of Organometallics*, Gelest, Inc. (1998), 612 William Leigh Drive, Tullytown, PA, 19007-6308.

[15] H. P. Klug and L. E. Alexander, *X-Ray Diffraction Procedures* (John Wiley and Sons, 1974), 2nd ed., figure 9-8.

[16] T. G. Fiske, Ph.D. thesis, University of California, Davis (1990), equation 3.31.

[17] R. Ruppin and R. Englman, Reports on Progress in Physics **33**, 149 (1970).

[18] W. L. Bragg and A. B. Pippard, Acta Crystallography **6**, 865 (1953).

[19] D. W. Berreman and F. C. Unterwald, Physical Review **174**, 791 (1968).

[20] J. L. Servoin and F. Gervais, Physical Review B **21**, 2038 (1980).

[21] F. Gervais and B. Piriou, Journal of Physics C: Solid State Physics **7**, 2374 (1974).

[22] R. Blinc and B. Zeks, *Soft Modes in Ferroelectrics and Antiferroelectrics* (North-Holland Publishing Company, 1974), appendix B.

[23] M. G. Cottam, D. R. Tilley, and B. Zeks, Journal of Physics C: Solid State Physics **17**, 1793 (1984), section 3.1.

[24] K. Binder, Ferroelectrics **35**, 99 (1981).

[25] V. L. Ginzburg, A. P. Levanyuk, and A. A. Sobyanin, Physics Reports **57**, 151 (1980), section 5.1.

[26] M. G. Cottam, D. R. Tilley, and B. Zeks, Journal of Physics C: Solid State Physics **17**, 1793 (1984), section 3.3.

[27] R. Shankar, *Principles of Quantum Mechanics* (Plenum Press, 1980), section 12.6.

[28] E. Fatuzzo and W. J. Merz, *Ferroelectricity* (John Wiley and Sons, Inc., 1967), page 110.

**Figures**

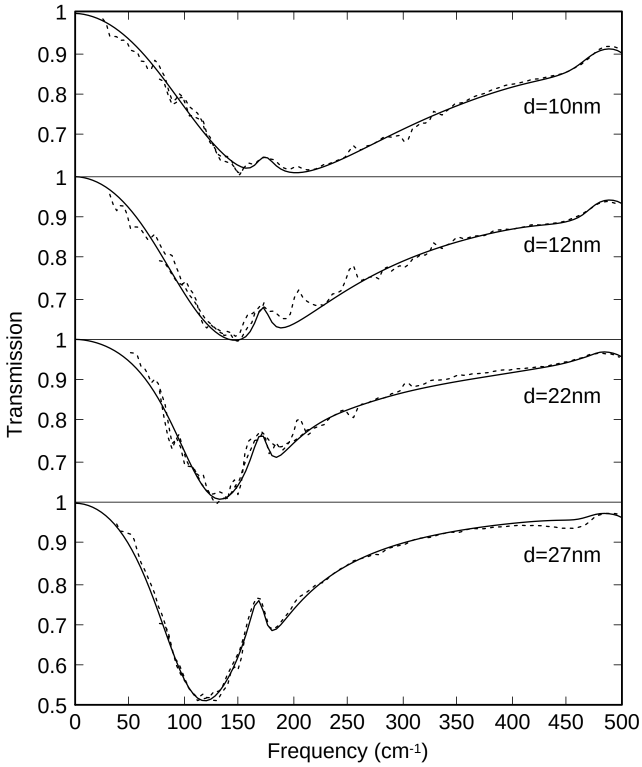


FIG. 1: Transmission spectra for the four samples discussed in the text. Dotted lines are data and solid lines are fits. The size of each sample is $d$. The large absorption feature corresponds to the soft mode.

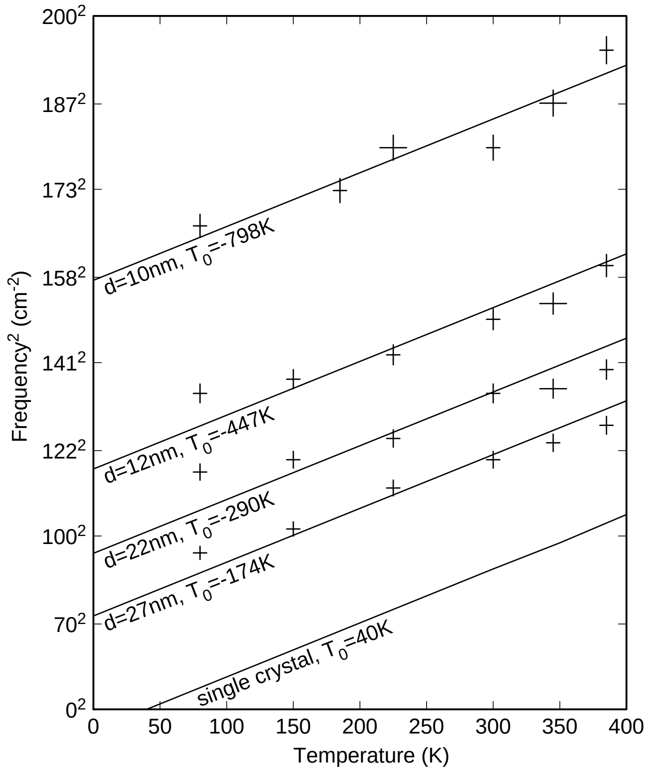


FIG. 2: Square of the soft mode frequency for four $SrTiO_3$ samples *vs.* temperature from 80 K to 385 K. The four upper straight lines are least square fits to $\omega_0^2 = A(T - T_0)$ for each sample keeping $A$ constant at its single crystal value and adjusting $T_0$. The bottom line shows single crystal behavior for comparison.

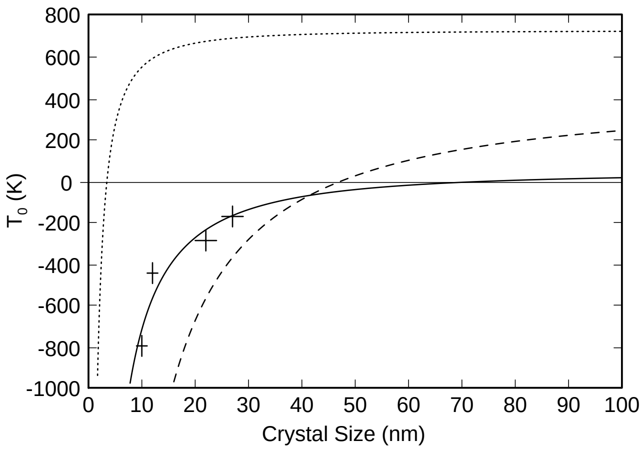


FIG. 3: Comparison of $T_0$ *vs.* particle size curves from Eq. (19) for $SrTiO_3$ (solid line) using our data and $BaTiO_3$ (dashed line) and $PbTiO_3$ (dotted line) using data from Zhong[10].

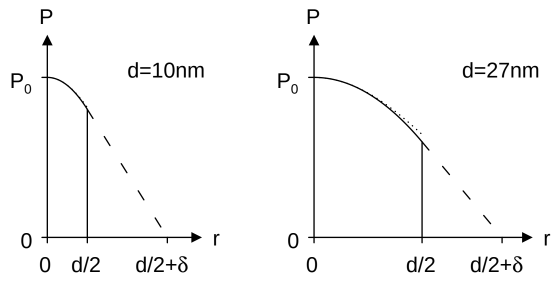


FIG. 4: Calculated radial polarization profiles for our smallest (left) and largest (right) crystal sizes. The solid line shows the Taylor approximation of Eq. (17). The dotted line shows the exact functional form $\sin ar/ar$ for the same $a$ as the Taylor approximation (hence its boundary condition is not exactly satisfied). The straight dashed line shows the graphical interpretation of the extrapolation length $\delta$.

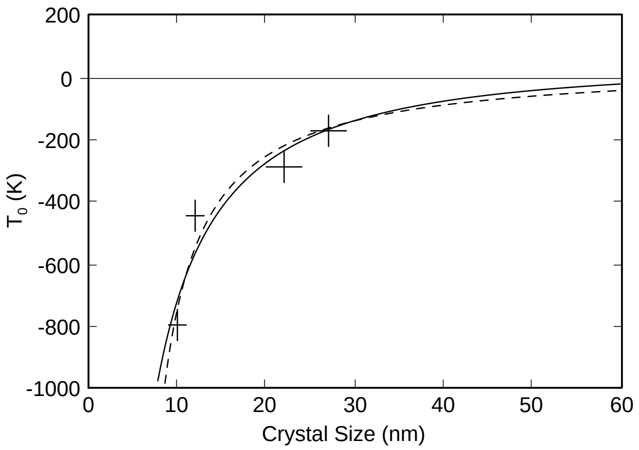


FIG. 5: Comparison of $T_0$ *vs.* particle size curves for the Landau model of Eq. (19), solid line, and the purely empirical model of Eq. (24), dashed line.